以碳量子點作為超解析螢光顯微鏡之閃爍發光團：從量子產率、發射光子數、工作週期、光穩定性到細胞染色之應用性

曾韋龍、林伯樵、張柏齡 國立中山大學 化學系

Abstract

This project aims to develop carbon quantum dot light-emitting materials that are highly stable, highly luminous, small in size (less than 5 nm), and self-luminous without additives. These materials will be used to solve the problem that the excitation light source 488 nm cannot be resolved in ultra-resolution imaging, and it is hoped that live cells can be imaged without additives to observe biological reactions within the cells. In the two-year project, we completed synthesizing and identifying carbon quantum dot materials and searched for suitable purification conditions. A highly water-soluble PEG polymer was used as the precursor material for the carbon quantum dots, and a high quantum yielding RhB dye was introduced into the synthesis process to enhance the properties of the carbon quantum dots. The carbon quantum dots with different quantum yields were successfully isolated and purified by RP-HPLC purification procedure.

Further analysis of the purified carbon quantum dots showed that one of the fractions had the best properties, including high quantum yields and superior fluorescent properties. This carbon quantum dot's morphology, chemical composition, and optical properties were determined using various analytical techniques. Time-resolved experiments confirmed the transformation of RhB and PEG during thermal reactions and the eventual formation of high-performance carbon quantum dots. Ultimately, the study also explores the potential of these carbon quantum dots for super-resolution imaging and live-cell imaging and provides detailed information on their efficacy in cell penetration and mitochondrial targeting. These results are expected to make carbon quantum dots a promising option for super-resolution imaging and bioimaging.

Reversible photoswitching of Alexa Fluor and ATTO dyes in the presence of thiols.

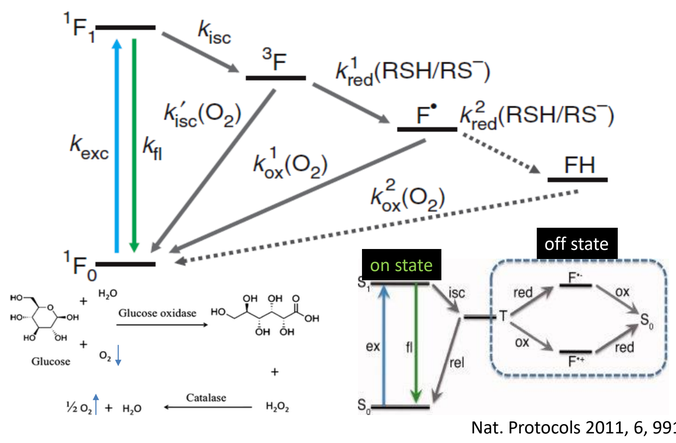

Nat. Protocols 2011, 6, 991.

Instrumentation of TIRF/HILO microscopy with IR-assisted z-axis stabilizer

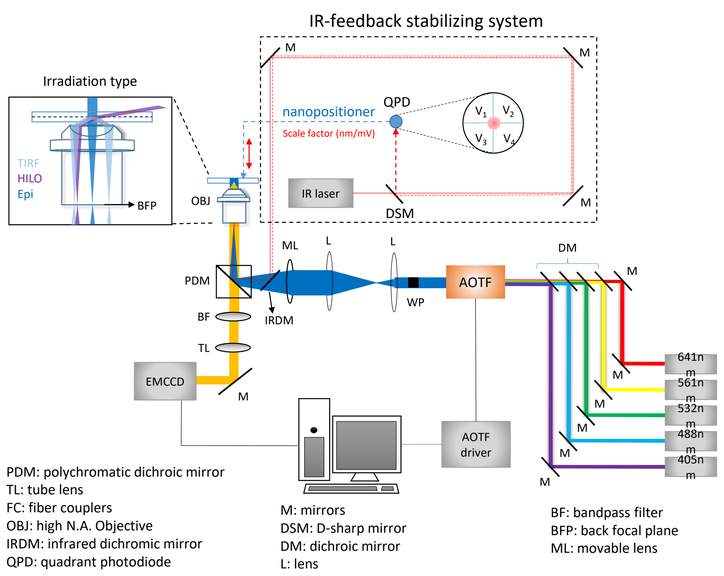

RP-HPLC purification of the CDs. (a) RP-HPLC chromatograms of the raw CD with six major labeled peaks. (b) Particle size and size distribution of the purified CDs in each fraction. (c) Absorption spectra of the purified PEG/RhB-CDs in each fraction. (d) Excitation-independent fluorescence spectra of the PEG/RhB-CDs-5. (e) Absolute quantum yields of the purified CDs in each fraction and their corresponding fluorescence lifetimes. (f) Photographs of the six fractions under UV light irradiation.

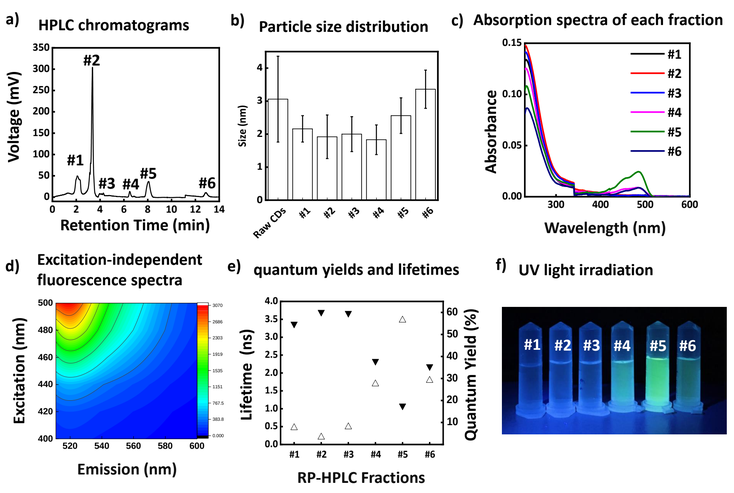

Characterization of the PEG/RhB-CDs-5. (A) High-resolution TEM image, (B) FT-IR spectrum, (C) 1H NMR spectrum, (D) 13C NMR spectrum, (E) XPS full spectrum, (F) high-resolution C1s XPS spectrum, and (G) high-resolution N1 XPS spectrum of the PEG/RhB-CDs-5. (A) Yellow circles indicate the location of PEG/RhB-CDs-5

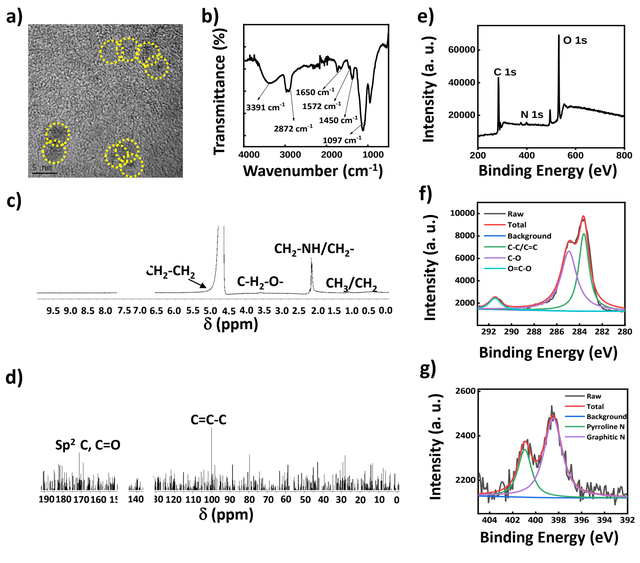

RP-UPLC/EIS-MS analysis of the intermediate products in the thermal reaction of RhB and PEG. Total ion chromatograms of the products formed from the reaction between RhB and PEG at 180 ˚C for (a) 0, (b) 10 min, (c) 20 min, and (d) 4 h.

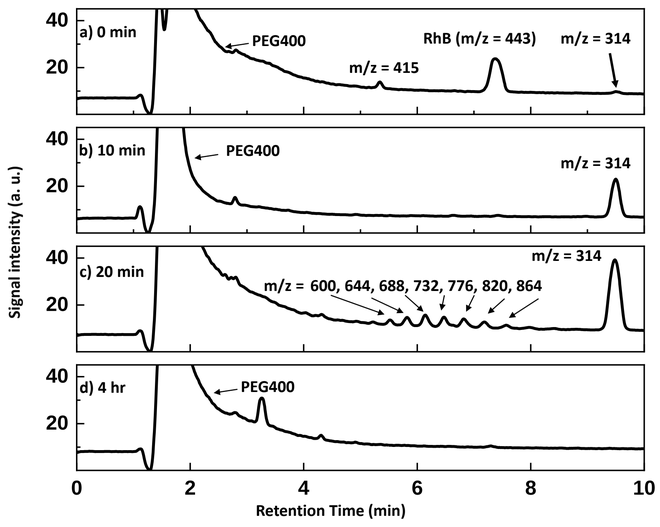

Schematic illustration of the proposed mechanism for the preparation of the raw PEG/RhB-CDs. The preparation of the raw PEG/RhB-CDs involves the thermal degradation of RhB, the esterification of PEG400 and DP314, the aggregation of the PEG-DP314 conjugates, and the carbonization of the aggregated conjugates

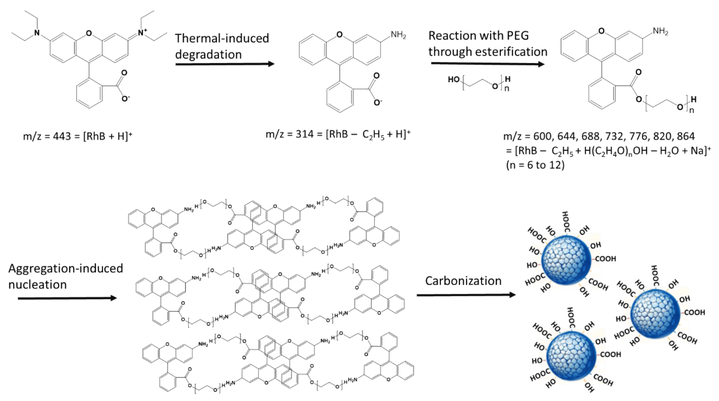

The effect of CDs concentration on the observation of individual CD photoblinking. The concentrations of CDs are a) 10 μg/mL, b) 1.0 μg/mL, c) 100 ng/mL, d) 10 ng/mL and e) 1.0 ng/mL respectively. The fluorescence can be observed by naked eye via projecting the laser beam (488 nm) through CDs solution (a) – c)) while single CD luminescence could be identified by EMCCD in all concentrations.

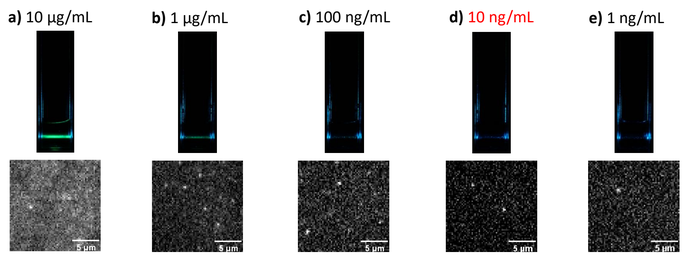

The photoblinking characteristics of Alexa Fluor 647, Alexa Fluor 488 and carbon dots in panel a) oxygen scavenger buffer and panel b) phosphate buffered saline. The images in panel a) and panel b) were 400th frames extracted from continuous TIRF imaging. The buffer effect on the on-state emitters with time is plotted in panel c).

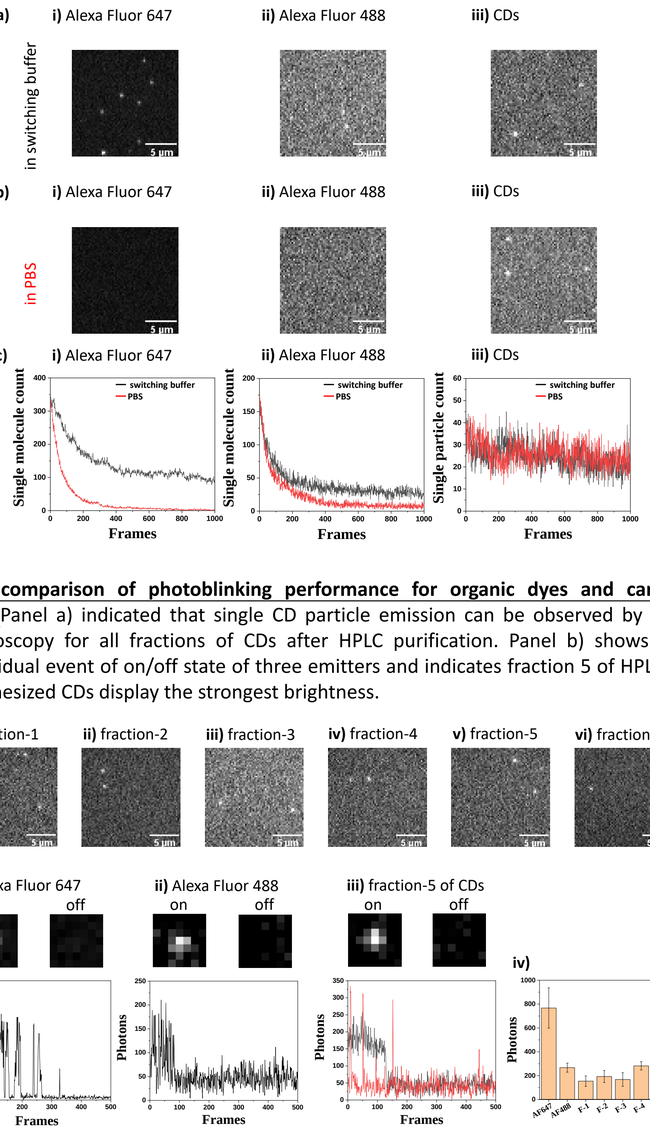

The comparison of photoblinking performance for organic dyes and carbon dots. Panel a) indicated that single CD particle emission can be observed by TIRF microscopy for all fractions of CDs after HPLC purification. Panel b) shows the individual event of on/off state of three emitters and indicates fraction 5 of HPLC of synthesized CDs display the strongest brightness.

The comparison of the point spread function for a) Alexa Fluor 647, b) Alexa Fluor 488 and c) CDs. The samples were dissolved in an oxygen scavenger buffer for a) and b); or PBS only for c). The samples were excited by laser beams (488 or 647 nm) with a radiant power at 50 mW laser projected under objective-type TIRF configuration. The images were obtained by an EMCCD with a 100x gain and exposure time of 50 milliseconds.

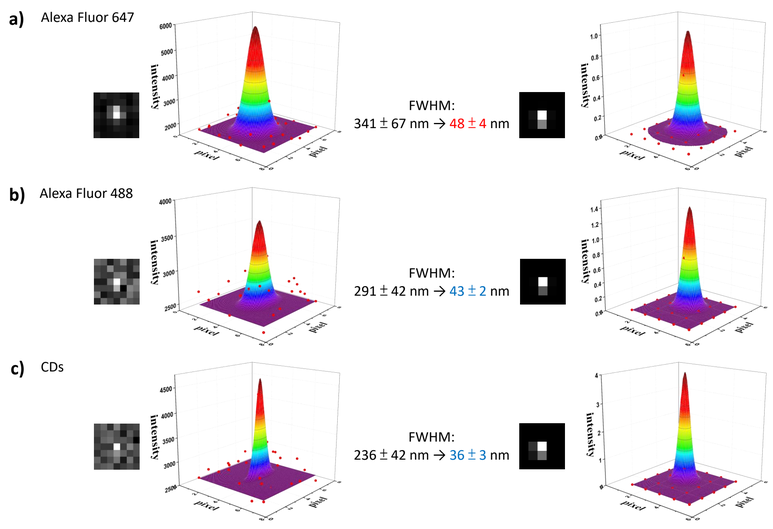

Testing of cell permeability of CDs. The cells were cultured on a TIRF microscope with a 37˚C, 5% CO_2 stage-top incubator. Panel a) To test the cell permeability we find the i) live cells by eyepiece followed by ii) add the fraction 5 CDs solution to the coverslip until the fluorescence reaches a steady state iii). The panel b shows the fluorescence increased with time and reached saturation in about 30 minutes.

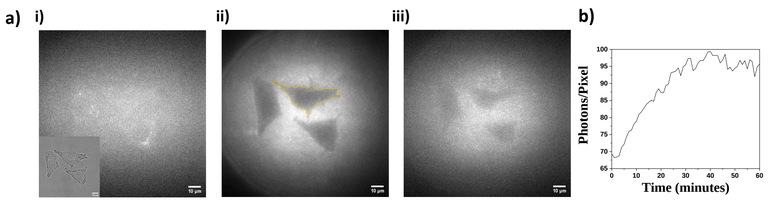

Time-lapse images for mitochondria staining by CDs-TPP and MitoTracker Green FM.
Panel a) The mitochondria maintain the sharp in CDs-TPP staining but morphology changed after MitoTracker Green FM staining as shown in panel b).

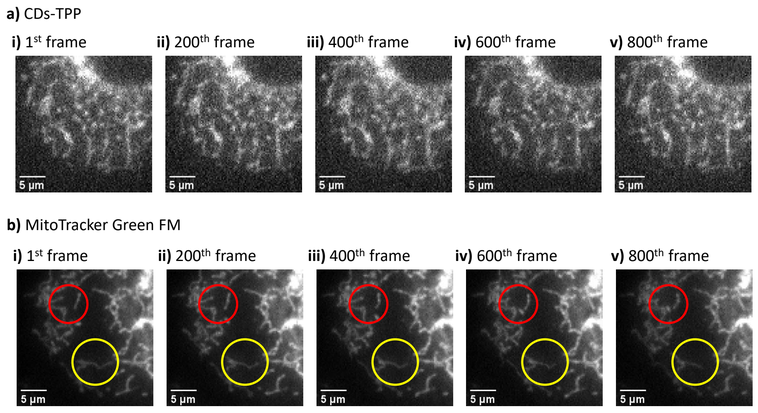

STORM imaging for mitochondria staining by CDs-TPP a) and CDs-SH-TPP b).
The fraction 5 CDs were conjugated by triphenylphosphonium (TPP) in order to stain mitochondria specifically. i) the CDs show unambiguous blinking of individual particles even through conjugation with TPP. ii) The live cell images after TTP-labeled CDs and iii) a zoon-in region from the cytoplasm of ii). iv) the ThunderSTORM images of iii) are compared to the HILO images in v). vi) a comparison of HILO image (single frames) and ThunderSTORM image (5000 frames) for the two adjacent mitochondria in iii)-iv) (yellow line).

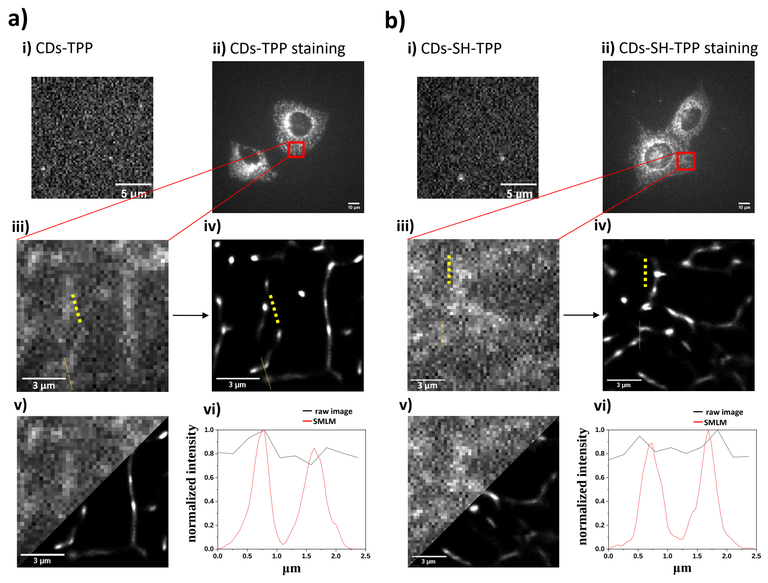

Summary

- A high-brightness carbon dot with great photostability has been synthesized by PEG and rhodamine B. The photoblinking of CDs persists for several minutes under strong laser illumination.
- The CDs show consistent photoblinking in the oxygen scavenger buffer and phosphate-buffered saline, allowing us to perform live cell staining without adding cytotoxic chemicals.
- The negatively charged surface of CDs makes it easier to modify organelle-specific ligands for live cell labeling with low cytotoxicity, therefore allowing us to label mitochondria in the simplest strategy.
- We demonstrated that the TPP-functionalized CDs can be transported into cells without any auxiliary chemicals. The transported TPP-CDs may specifically target to mitochondria and serve as a single emitter for STORM imaging.
- We also find that the mitochondria stained by TPP-CDs show less change in morphology as compared to those stained by MitoTracker Green FM. Based on this, the less moving emitters provide more reliable images over several minutes for reconstruction by ThunderSTORM and produce fine mitochondria images for live cell.